Molecular Phylogenetics and Evolution 83 (2015) 278–292

Contents lists available at ScienceDirect

Molecular Phylogenetics and Evolution

journal homepage: www.elsevier.com/locate/ympev

Phylogenetic and transcriptomic analyses reveal the evolution of bioluminescence and light detection in marine deep-sea shrimps of the family Oplophoridae (Crustacea: Decapoda)

Juliet M. Wong [a,*], Jorge L. Pérez-Moreno [a], Tin-Yam Chan [b], Tamara M. Frank [c], Heather D. Bracken-Grissom [a]

[a] Florida International University, Department of Biological Sciences, 3000 NE 151st St, North Miami, FL 33181, United States
[b] Institute of Marine Biology and Center of Excellence for the Oceans, National Taiwan Ocean University, Keelung 20224, Taiwan, ROC
[c] Nova Southeastern University, Oceanographic Center, 8000 North Ocean Drive, Dania Beach, FL 33004, United States

ARTICLE INFO

Article history:
Received 2 September 2014
Revised 17 November 2014
Accepted 22 November 2014
Available online 4 December 2014

Keywords:
Photophores
Shrimp
Bioluminescence
RNA-seq
Opsins
Ultraviolet

ABSTRACT

Bioluminescence is essential to the survival of many organisms, particularly in the deep sea where light is limited. Shrimp of the family Oplophoridae exhibit a remarkable mechanism of bioluminescence in the form of a secretion used for predatory defense. Three of the ten genera possess an additional mode of bioluminescence in the form of light-emitting organs called photophores. Phylogenetic analyses can be useful for tracing the evolution of bioluminescence, however, the few studies that have attempted to reconcile the relationships within Oplophoridae have generated trees with low-resolution. We present the most comprehensive phylogeny of Oplophoridae to date, with 90% genera coverage using seven genes (mitochondrial and nuclear) across 30 oplophorid species. We use our resulting topology to trace the evolution of bioluminescence within Oplophoridae. Previous studies have suggested that oplophorid visual systems may be tuned to differentiate the separate modes of bioluminescence. While all oplophorid shrimp possess a visual pigment sensitive to blue-green light, only those bearing photophores have an additional pigment sensitive to near-ultraviolet light. We attempt to characterize opsins, visual pigment proteins essential to light detection, in two photophore-bearing species (*Systellaspis debilis* and *Oplophorus gracilirostris*) and make inferences regarding their function and evolutionary significance.

1. Introduction

Bioluminescence, the production of light by a living organism, is a captivating phenomenon that can be found in a variety of forms and across a wide range of taxa. The general mechanism of bioluminescence involves the oxidation of a light-emitting molecule (a luciferin) by an enzyme catalyst (a luciferase or photoprotein) (Haddock et al., 2010). Not only is there a wide array of enzyme luciferases, but there can be enormous variability in the wavelengths of emitted light, specialized bioluminescent organs or bioluminescent bacteria within certain organisms, behavioral and functional applications of the light, as well as the bioluminescent organisms themselves (Wilson and Hastings, 2013). The study of bioluminescence has gained attention due to its applications in environmental monitoring (Steinberg et al., 1995), biotechnology and medicine (Roda et al., 2004), and even agriculture and food safety (Gracias and McKillip, 2004). Even though terrestrial representatives occur, the vast majority of bioluminescent taxa have been found widely distributed throughout Earth's oceans and throughout the water column (Haddock et al., 2010). The predominance of light-producing organisms in the sea illustrates the importance of bioluminescence to animal function, behavior, predator–prey interactions and communication. Bioluminescence has been estimated to have evolved 40–50 or more times among extant taxa, additionally suggesting that the ability to produce light is advantageous to many organisms (Haddock et al., 2010). Bioluminescence is particularly important in the deep sea where, with the exception of some dim, downwelling sunlight, bioluminescence is the only source of light (Herring, 1983; Latz et al.,

Abbreviations: SWS, short-wavelength-sensitive; LWS, long-wavelength-sensitive; ML, maximum likelihood; BAY, Bayesian; ASR, ancestral state reconstruction; BP, bootstrap; PP, posterior probability.

* Corresponding author.
E-mail addresses: julietmwong@gmail.com (J.M. Wong), jorge.perezmoreno@fiu.edu (J.L. Pérez-Moreno), tychan@mail.ntou.edu.tw (T.-Y. Chan), tfrank1@nova.edu (T.M. Frank), hbracken@fiu.edu (H.D. Bracken-Grissom).

http://dx.doi.org/10.1016/j.ympev.2014.11.013
1055-7903/

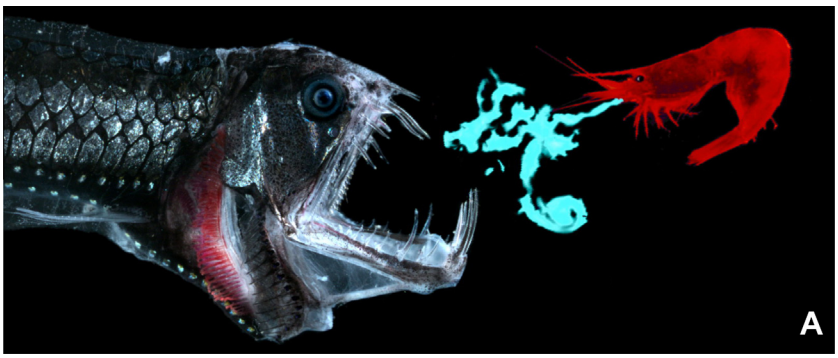

Fig. 1A. Composite showing *Acanthephyra purpurea* exhibiting secretory luminescence as a defensive mechanism in response to a viperfish, *Chauliodus danae*. Photograph by Edith Widder.

1988; Widder et al., 1983). Unfortunately, bioluminescence in the deep sea is greatly understudied due largely to the difficulties associated with conducting observational research at great depths, and to the challenges associated with collecting specimens without damaging them as they are brought to the surface.

Deep-sea shrimp of the family Oplophoridae Dana, 1852a (Crustacea: Decapoda: Caridea) exhibit a remarkable mechanism of bioluminescence in the form of a blue luminescent spew that likely originates in the hepatopancreas and is secreted from the mouth (Herring, 1976, 1985) (Fig. 1A). This luminescent secretion is hypothesized to be a defensive mechanism used when the shrimp is distressed as a means of startling or distracting potential predators (Herring, 1976). In addition to secretory luminescence, three oplophorid genera possess a second mechanism of bioluminescence in the form of cuticular photophores (Fig. 1B). Photophores are complex light-emitting organs composed of bioluminescent cells (photocytes) as well as reflectors, lenses, and filter structures capable of altering the spectral distribution, angular distribution, and direction or intensity of the light emitted (Denton et al., 1972, 1985; Herring, 1996; Nowel et al., 1998). Photophores are believed to function in counter-illumination by mimicking downwelling light, thereby disrupting the shrimp's silhouette that would otherwise be detectable from below by predators (Nowel et al., 1998). Coelenterazine, the only luciferin known to occur in luminescent decapod crustaceans, is used in both oplophorid secretory and photophore bioluminescence, though coelenterazine levels in the secretion are nearly three orders of magnitude greater than what is found in photophores (Shimomura et al., 1980; Thomson et al., 1995).

Oplophorid shrimp have a cosmopolitan distribution, though none are found in polar regions (Chace, 1986; Chan et al., 2010). Recently, Oplophoridae was split into two families, Acanthephyridae and Oplophoridae (Chan et al., 2010; De Grave and Fransen, 2011). However, we provide evidence that oplophorid shrimp are monophyletic, and have therefore chosen to follow an earlier classification that combines all ten extant genera within the single family of Oplophoridae (De Grave et al., 2009). Oplophorids of the genera *Systellaspis*, *Janicella*, and *Oplophorus* possess secretory luminescence as well as cuticular photophores, while all other genera (*Acanthephyra*, *Ephyrina*, *Heterogenys*, *Meningodora*, *Notostomus*, *Hymenodora*, and *Kemphyra*) possess only secretory luminescence and completely lack cuticular photophores (Chan et al., 2010; Nowel et al., 1998). Tracing the different modes of luminescence through a phylogeny can be a useful means of investigating the evolution of bioluminescence in oplophorid shrimp. Unfortunately, the few studies to have attempted a phylogenetic analysis of Oplophoridae spanned only six to ten out of 71 different oplophorid species and included only 18S nuclear and 16S mitochondrial genes, which provided topologies of low resolution (Bracken et al., 2009; Chan et al., 2010). Here, we present the most comprehensive phylogenetic analyses of Oplophoridae to date, spanning 30 oplophorid species with 90% genera coverage, and including data from seven different genes. We then use the resulting phylogeny to trace the evolution of the two modes of bioluminescence throughout the family.

Oplophorid shrimp have been shown to possess interesting visual characteristics that may be associated with their multiple forms of bioluminescence. All oplophorid genera appear to have

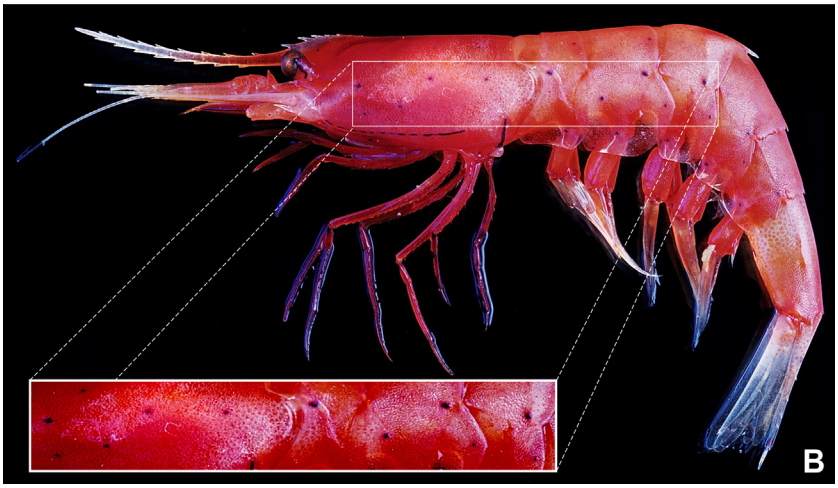

Fig. 1B. Close-up and full lateral view of *Systellaspis debilis* showing multiple cuticular photophores. Photograph by Tin-Yam Chan.

a photopigment in their eyes with a maximum sensitivity in the blue-green spectrum (490–510 nm) (Frank and Case, 1988; Frank and Widder, 1994a). However, some photophore-bearing species (within *Systellaspis*, *Oplophorus*, and *Janicella*) bear an additional photopigment that has a spectral sensitivity maxima in the near-ultraviolet (UV) spectrum (390–410 nm) (Cronin and Frank, 1996; Frank and Case, 1988; Frank and Widder, 1994a,b; Gaten et al., 2004). For instance, photoreceptors of *Notostomus gibbosus* and *N. elegans* have a sensitivity maximum at 490 nm and photoreceptors of *Acanthephyra smithi* and *A. curtirostris* have a sensitivity maximum at 510 nm (Frank and Case, 1988). However, photoreceptors of photophore-bearing species *Janicella spinicauda*, *Systellaspis debilis*, *Oplophorus spinosus*, and *O. gracilirostris* have sensitivity maxima at both 500 nm (blue-green) and 400 nm (near-UV) (Cronin and Frank, 1996; Frank and Case, 1988). Because photophore luminescence of *Systellaspis*, *Oplophorus*, and *Janicella* has a substantially narrower spectral distribution than that of the secretory luminescence of the same individual, it has been suggested that the presence of both blue-green and near-UV-sensitive visual pigments provides these shrimps with the ability to differentiate between their different modes of bioluminescence (Frank and Case, 1988; Gaten et al., 2004). This capability would play an important role in congener recognition, communication, and predator discrimination (Cronin and Frank, 1996; Frank and Case, 1988; Frank and Widder, 1994a).

While behavioral and morphological studies have been conducted to examine the photopigments within oplophorid eyes and their visual sensitivities, there have been no genetic analyses conducted in an attempt to characterize the visual genes controlling light detection. Here, we investigate RNA-seq data from two photophore-bearing oplophorid species, *S. debilis* and *O. gracilirostris*, and present the first examination of genes involved in the detection of light within oplophorid shrimp. We include a benthic penaeid shrimp, *Benthesicymus bartletti* Smith, 1882, which is not known to be bioluminescent, to aid in this comparison. We specifically examine opsins, proteins involved in phototransduction (the conversion of light into electrical signals), that when bound to a chromophore, form photopigments that are fundamental to the detection of light (Porter et al., 2011; Wald, 1968). Opsin proteins control the wavelength sensitivity of visual pigments, and certain amino acid substitutions in opsin sequences have been shown to alter wavelength specificity (Carleton and Kocher, 2001). In accordance with previous arthropod opsin studies, we have chosen to define visual pigment photosensitivities as short-wavelength-sensitive, SWS (shorter than 490 nm, UV to blue), and long-wavelength-sensitive, LWS (longer than 490 nm, blue-green to red) (Briscoe and Chittka, 2001; Henze et al., 2012; Kitamoto et al., 1998; Porter et al., 2007). We hypothesize that the genes for opsins forming blue-green and near-UV-sensitive visual pigments are expressed within the eyes of photophore-bearing genera, and that these visual pigments may allow them to better distinguish between different forms of light, such as surrounding ambient light and their two modes of bioluminescence.

2. Materials and methods

2.1. Taxon sampling

A total of 82 oplophorid shrimp spanning 30 different species were used in this study (Table 1). Nine of the ten oplophorid genera were included (*Oplophorus*, *Systellaspis*, *Janicella*, *Acanthephyra*, *Ephyrina*, *Heterogenys*, *Meningodora*, *Notostomus*, *Hymenodora*). The remaining genus, *Kemphyra*, was unavailable for molecular analysis. *Kemphyra* consists of one species, *K. corallina*, and is thought to be a rare genus that is predominantly benthic, ranging in depth from 1000 to greater than 2700 m (Chace, 1986). Specimens were collected from sites in the Gulf of Mexico, the North Atlantic Ocean (in proximity to the Mid-Atlantic Ridge between the Azores and Iceland), Spain, Vietnam, the Philippines, and Taiwan (Table 1). Eleven specimens spanning five different families outside Oplophoridae were chosen as outgroup taxa after preliminary analyses (see results). These outgroup representatives included a benthesicymid (*Gennadas valens*), a penaeid (*Funchalia villosa*), two pasiphaeids (*Glyphus marsupialis* and *G. aff. marsupialis*), a pandalid (*Heterocarpus ensifer*), and two nematocarcinids (*Nematocarcinus cursor* and *N. gracilis*) (Table 1). All specimens and/or tissue samples were either frozen at −80 °C or stored in 70% ethanol.

2.2. Gene selection

We selected seven genes for these analyses in an attempt to maximize the resolution of our phylogeny. Specifically, we included mitochondrial ribosomal genes (12S and 16S), a mitochondrial protein-coding gene (cytochrome c oxidase subunit I, COI), nuclear ribosomal genes (18S and 28S), and nuclear protein-coding genes (histone H3 and sodium–potassium ATPase α-subunit, NaK). These genes have proved to be useful in species- to family-level relationships across decapods (Bracken-Grissom et al., 2013, 2014; Tsang et al., 2008).

2.3. DNA extraction, PCR, and sequencing

Genomic DNA was extracted from muscle tissue of the abdomen or pleopods using the Qiagen DNeasy® Blood and Tissue Kit (Cat. No. 69506) following the manufacturer's instructions. One or more sets of primers were chosen to amplify up to seven different gene regions using polymerase chain reaction (PCR) (see Supplementary Table S1). The following gene regions were targeted for sequencing: 16S large ribosomal subunit (~550 bp, Crandall and Fitzpatrick, 1996; Palumbi et al., 1991; Palumbi, 1996; Schubart et al., 2002), 12S small ribosomal subunit (~400 bp, Buhay et al., 2007), cytochrome oxidase 1 (COI) protein-coding gene (~650 bp, Folmer et al., 1994), 28S large ribosomal subunit (~2500 bp, Toon et al., 2009; Whiting, 2002), 18S small ribosomal subunit (~1800 bp, Apakupakul et al., 1999; Whiting, 2002; Whiting et al., 1997), protein-coding histone 3 (H3) (~350 bp, Colgan et al., 1998), and protein-coding sodium–potassium ATPase α-subunit (NaK) (~630 bp, Tsang et al., 2008).

PCR amplification reactions were performed in 26 μL volumes containing 2 μL of DNA template, 6.45 μL of sterile non-DEPC treated water, 5 μL of 5× combinatorial PCR enhancer solution (CES) (Ralser et al., 2006), 3 μL of 2 mM deoxyribonucleotide triphosphate mix (dNTPs), 2.5 μL of 10× PCR Buffer, 2.3 μL of 5 M betaine, 2 μL of each 10 μM forward and reverse primer, and 1.5 μL of 0.1 g/mL bovine serum albumin (BSA). 12S, 16S, 18S, 28S, and H3 thermal cycling profiles included an initial denaturation of 1 min at 94 °C, followed by 35 cycles of 30 s at 94 °C, 30 s at 46–58 °C (depending on gene region), 1 min at 72 °C, and then a final extension of 10 min at 72 °C. The COI thermal cycling profile included an initial denaturation of 1 min at 94 °C, followed by 35–40 cycles of 1 min at 94 °C, 1 min at 40 °C, 1.5 min at 72 °C, and then a final extension of 7 min at 72 °C (Folmer et al., 1994). The NaK thermal cycling profile included an initial denaturation of 1 min at 94 °C, followed by 35–40 cycles of 30 s at 94 °C, 30 s at 55–60 °C (depending on species), 1.5 min at 72 °C, and then a final extension of 10 min at 72 °C (Ma et al., 2009). Unpurified PCR products were sent to Beckman Coulter Genomics (Danvers, MA, USA) for purification using solid-phase reversible immobilization (SPRI) technology, sequencing using BigDye Terminator v3.1, post reaction dye terminator removal using Agencourt CleanSEQ, and sequence

Table 1
Oplophoridae and outgroup individuals used in phylogenetic reconstruction with localities, voucher numbers, and GenBank accession numbers.

Species	Locality	Voucher no.	12S	16S	COI	18S	28S	H3	NaK
Family Benthesicymidae Wood-Mason in Wood-Mason & Alcock, 1891a									
Gennadas Spence Bate, 1881									
G. valens (Smith, 1884)	Gulf of Mexico	HBG1132A	KP076015	N/A	N/A	N/A	N/A	KP076142	KP076051
Family Nematocarcinidae Smith, 1884									
Nematocarcinus A. Milne-Edwards, 1881b									
N. cursor A. Milne-Edwards, 1881	Gulf of Mexico	HBG554	KP075997	KP075928	N/A	KP075826	KP075760	KP076132	N/A
N. gracilis Spence Bate, 1888	N/A	HBG397	KP075996	KP075927	N/A	KP075825	KP075759	KP076131	N/A
Family Oplophoridae Dana, 1852a									
Acanthephyra[s] A. Milne-Edwards, 1881b									
A. acutifrons Spence Bate, 1888	Gulf of Mexico	HBG1149B	KP075954	KP075876	KP076169	KP075799	KP075724	KP076085	N/A
A. acutifrons Spence Bate, 1888	Gulf of Mexico	HBG1157	KP075951	KP075878	N/A	KP075829	KP075725	KP076082	KP076040
A. acutifrons Spence Bate, 1888	Gulf of Mexico	HBG1254	KP075955	KP075874	KP076167	KP075817	KP075727	KP076084	KP076037
A. acutifrons Spence Bate, 1888	Gulf of Mexico	HBG1265	KP075952	KP075877	N/A	KP075785	KP075726	KP076083	KP076036
A. acutifrons Spence Bate, 1888	Taiwan	NTOU M01840	KP075953	KP075875	KP076168	KP075790	KP075728	KP076081	N/A
A. armata A. Milne-Edwards, 1881	Vietnam	HBG919	KP075962	KP075894	N/A	KP075786	KP075739	KP076091	N/A
A. carinata Spence Bate, 1888	Philippines	NTOU M01841	KP075969	KP075896	KP076184	KP075798	KP075737	KP076093	N/A
A. cucullata Faxon, 1893	Taiwan	NTOU M01843	KP075935	KP075893	KP076160	KP075809	KP075736	KP076110	N/A
A. curtirostris Wood-Mason & Alcock, 1891	Gulf of Mexico	HBG1255	KP075956	N/A	KP076163	KP075793	KP075732	KP076087	KP076028
A. curtirostris Wood-Mason & Alcock, 1891	Gulf of Mexico	HBG1263	KP075957	KP075890	KP076165	KP075804	KP075730	KP076112	N/A
A. curtirostris Wood-Mason & Alcock, 1891	Gulf of Mexico	HBG1407	KP075958	KP075889	KP076161	KP075807	KP075734	KP076088	KP076029
A. curtirostris Wood-Mason & Alcock, 1891	Gulf of Mexico	HBG819	KP075960	KP075891	KP076162	KP075820	KP075729	KP076111	KP076041
A. curtirostris Wood-Mason & Alcock, 1891	Gulf of Mexico	HBG1155A	KP075959	KP075888	KP076164	KP075816	KP075731	KP076113	N/A
A. eximia Smith, 1884	N/A	HBG399	N/A	KP075897	N/A	KP075823	KP075744	KP076125	N/A
A. fimbriata Alcock & Anderson, 1894	Philippines	NTOU M01844	KP075961	KP075895	KP076185	KP075788	KP075738	KP076092	N/A
A. media Spence Bate, 1888	Philippines	NTOU M01845	KP075937	KP075892	KP076166	KP075805	KP075733	KP076086	N/A
A. pelagica (Risso, 1816)	Gulf of Mexico	HBG1242	KP075938	KP075879	KP076181	KP075796	KP075721	KP076108	KP076021
A. pelagica (Risso, 1816)	Gulf of Mexico	HBG1250A	KP075940	N/A	KP076179	KP075822	KP075714	KP076090	N/A
A. pelagica (Risso, 1816)	Gulf of Mexico	HBG1406	KP075939	KP075881	KP076180	KP075808	KP075722	KP076089	KP076022
A. pelagica (Risso, 1816)	North Atlantic	HBG153	KP075941	KP075880	KP076182	KP075789	KP075715	KP076100	KP076027
A. purpurea A. Milne-Edwards, 1881	Gulf of Mexico	HBG1125	KP075945	N/A	KP076176	KP075773	KP075711	KP076102	N/A
A. purpurea A. Milne-Edwards, 1881	Gulf of Mexico	HBG1152	KP075949	N/A	KP076173	KP075811	KP075718	KP076096	N/A
A. purpurea A. Milne-Edwards, 1881	North Atlantic	HBG1165	KP075936	KP075899	KP076174	KP075812	KP075720	KP076101	KP076026
A. purpurea A. Milne-Edwards, 1881	Spain	HBG1166	KP075948	N/A	KP076175	KP075814	KP075713	KP076109	KP076024
A. purpurea A. Milne-Edwards, 1881	Gulf of Mexico	HBG1269	KP075944	KP075884	KP076171	KP075794	KP075723	KP076097	N/A
A. purpurea A. Milne-Edwards, 1881	Gulf of Mexico	HBG899A	KP075942	KP075882	KP076170	KP075782	KP075719	KP076095	KP076023
A. purpurea A. Milne-Edwards, 1881	Gulf of Mexico	HBG900	KP075946	KP075885	KP076177	KP075781	KP075717	KP076098	N/A
A. purpurea A. Milne-Edwards, 1881	North Atlantic	HBG157	KP075950	KP075887	N/A	KP075819	KP075716	KP076127	N/A
A. purpurea A. Milne-Edwards, 1881	Gulf of Mexico	HBG899B	KP075943	KP075883	KP076172	N/A	KP075710	KP076094	N/A
A. quadrispinosa Kemp, 1939	Taiwan	NTOU M01846	KP075947	KP075886	KP076178	KP075821	KP075712	KP076099	KP076025
Ephyrina[s] Smith, 1885a									
E. bifida Stephensen, 1923	North Atlantic	HBG160	KP075970	N/A	KP076186	KP075779	KP075754	N/A	KP076039
E. figueirai Crosnier & Forest, 1973	Spain	HBG1176A	KP075967	KP075913	KP076190	KP075815	KP075753	KP076103	N/A

(*continued on next page*)

Table 1 (*continued*)

Species	Locality	Voucher no.	12S	16S	COI	18S	28S	H3	NaK
E. figueirai Crosnier & Forest, 1973	Spain	HBG1176B	KP075968	KP075912	KP076191	KP075818	KP075752	KP076104	N/A
E. figueirai spinicauda Lin & Chan, 2001	Taiwan	NTOU M01847	KP075966	KP075911	KP076189	KP075800	KP075751	KP076105	KP076038
E. ombango Crosnier & Forest, 1973	Gulf of Mexico	HBG1230	KP075964	KP075914	KP076188	KP075802	KP075755	KP076107	N/A
E. ombango Crosnier & Forest, 1973	Taiwan	NTOU M01848	KP075965	KP075915	KP076187	KP075810	KP075750	KP076106	N/A
Heterogenys[S] Chace, 1986									
H. microphthalma (Smith, 1885)	Taiwan	NTOU M01849	KP075963	KP075898	KP076183	KP075787	KP075735	KP076124	KP076035
Hymenodora[S] G.O. Sars, 1877									
H. glacialis (Buchholz, 1874)	N/A	HBG84	KP076020	KP075908	N/A	KP075828	KP075756	KP076133	N/A
H. gracilis Smith, 1886	North Atlantic	HBG96	KP076019	KP075909	N/A	KP075827	KP075758	KP076134	KP076048
Janicella[P] Chace, 1986									
J. spinicauda (A. Milne-Edwards, 1883)	Taiwan	HBG1596	KP076018	KP075934	N/A	N/A	N/A	KP076129	N/A
J. spinicauda (A. Milne-Edwards, 1883)	Gulf of Mexico	HBG905	N/A	KP075932	N/A	KP075856	N/A	KP076128	N/A
J. spinicauda (A. Milne-Edwards, 1883)	Taiwan	HBG946	KP076017	KP075933	N/A	KP075858	N/A	KP076130	N/A
Meningodora[S] Smith, 1882									
M. mollis Smith, 1882	Spain	HBG1170	KP075977	N/A	KP076193	KP075813	KP075741	KP076116	KP076034
M. mollis Smith, 1882	Gulf of Mexico	HBG901	KP075978	KP075910	KP076192	KP075783	KP075742	KP076115	KP076033
M. mollis Smith, 1882	Taiwan	NTOU M01850	KP075979	N/A	N/A	KP075792	KP075740	KP076123	N/A
M. vesca (Smith, 1886)	Gulf of Mexico	HBG1241	KP075980	KP075907	N/A	KP075791	KP075743	KP076114	N/A
Notostomus[S] A. Milne-Edwards, 1881b									
N. elegans A. Milne-Edwards, 1881	Gulf of Mexico	HBG1127	KP075975	N/A	KP076195	KP075806	KP075745	KP076118	N/A
N. elegans A. Milne-Edwards, 1881	Gulf of Mexico	HBG1153	KP075971	KP075903	N/A	KP075801	KP075764	KP076121	N/A
N. elegans A. Milne-Edwards, 1881	Spain	HBG1169	KP075972	KP075904	N/A	KP075780	KP075747	KP076117	KP076032
N. elegans A. Milne-Edwards, 1881	Gulf of Mexico	HBG1232	KP075973	KP075900	KP076194	KP075803	KP075746	KP076119	N/A
N. elegans A. Milne-Edwards, 1881	Gulf of Mexico	HBG902	KP075974	KP075901	N/A	KP075797	KP075748	KP076122	KP076031
N. elegans A. Milne-Edwards, 1881	Gulf of Mexico	ULLZ11481	KP075976	KP075906	N/A	KP075824	KP075757	KP076126	N/A
N. gibbosus A. Milne-Edwards, 1881	Gulf of Mexico	HBG903A	N/A	KP075905	N/A	KP075795	KP075749	KP076120	KP076030
Oplophorus[P] H. Milne Edwards, 1837 [in H. Milne Edwards, 1834–1840]									
O. gracilirostris A. Milne-Edwards, 1881	Gulf of Mexico	HBG1128C	KP075988	N/A	KP076155	KP075832	KP075703	KP076071	N/A
O. gracilirostris A. Milne-Edwards, 1881	Gulf of Mexico	HBG1135	KP075986	N/A	KP076157	KP075834	KP075704	KP076052	N/A
O. gracilirostris A. Milne-Edwards, 1881	Gulf of Mexico	HBG754	KP075985	KP075919	KP076154	KP075830	KP075699	KP076067	N/A
O. gracilirostris A. Milne-Edwards, 1881	Gulf of Mexico	HBG904A	KP075991	KP075922	KP076151	KP075848	KP075701	KP076066	KP076045
O. gracilirostris A. Milne-Edwards, 1881	Gulf of Mexico	HBG906A	KP075982	KP075917	KP076153	KP075849	KP075698	KP076070	KP076046
O. gracilirostris A. Milne-Edwards, 1881	Gulf of Mexico	HBG907	KP075983	KP075918	KP076156	KP075840	KP075700	KP076069	KP076044
O. gracilirostris A. Milne-Edwards, 1881	Gulf of Mexico	HBG908	KP075984	KP075921	KP076152	KP075833	KP075702	KP076065	N/A
O. gracilirostris A. Milne-Edwards, 1881	Gulf of Mexico	HBG909A	KP075987	KP075920	KP076150	KP075847	KP075697	KP076072	N/A
O. spinosus (Brullé, 1839)	Spain	HBG1168A	KP075989	N/A	KP076149	KP075842	KP075706	KP076074	N/A
O. spinosus (Brullé, 1839)	Spain	HBG1168B	KP075990	N/A	KP076148	KP075841	KP075705	KP076073	N/A
O. typus H. Milne Edwards, 1837 [in H. Milne Edwards, 1834–1840]	Vietnam	HBG941	KP075981	KP075923	KP076158	KP075835	KP075765	KP076068	N/A
Systellaspis[P] Spence Bate, 1888									
S. braueri braueri (Balss, 1914a)	North Atlantic	HBG91	KP075995	KP075926	KP076212	KP075853	KP075709	KP076078	N/A
S. curvispina Crosnier, 1987	Taiwan	NTOU M01851	KP075994	KP075916	KP076159	KP075784	N/A	KP076064	N/A
S. debilis (A. Milne-Edwards, 1881)	Gulf of Mexico	HBG1126C	KP076000	KP075873	KP076205	KP075851	KP075688	KP076076	N/A
S. debilis (A. Milne-Edwards, 1881)	Spain	HBG1161	KP076008	KP075870	KP076210	KP075845	KP075689	KP076060	N/A
S. debilis (A. Milne-Edwards, 1881)	Spain	HBG1163	KP076009	KP075869	KP076203	KP075844	KP075690	KP076062	N/A

Table 1 (*continued*)

Species	Locality	Voucher no.	12S	16S	COI	18S	28S	H3	NaK
S. debilis (A. Milne-Edwards, 1881)	Gulf of Mexico	HBG1204	KP076001	KP075862	KP076201	KP075839	KP075684	KP076055	N/A
S. debilis (A. Milne-Edwards, 1881)	Gulf of Mexico	HBG1270A	KP075999	KP075872	KP076207	KP075831	KP075692	KP076061	N/A
S. debilis (A. Milne-Edwards, 1881)	Gulf of Mexico	HBG1270B	KP076003	KP075860	KP076208	KP075843	KP075691	KP076075	KP076043
S. debilis (A. Milne-Edwards, 1881)	Gulf of Mexico	HBG1283	KP076002	KP075864	KP076204	N/A	KP075696	KP076054	N/A
S. debilis (A. Milne-Edwards, 1881)	Gulf of Mexico	HBG753	KP075998	KP075859	KP076200	KP075836	KP075687	KP076057	N/A
S. debilis (A. Milne-Edwards, 1881)	Gulf of Mexico	HBG910	KP076010	KP075871	KP076209	KP075837	KP075685	KP076056	KP076042
S. debilis (A. Milne-Edwards, 1881)	Gulf of Mexico	HBG911A	KP076011	KP075863	KP076202	KP075850	KP075686	KP076053	N/A
S. debilis (A. Milne-Edwards, 1881)	Gulf of Mexico	HBG913	KP076007	KP075868	KP076206	KP075838	KP075694	KP076059	N/A
S. debilis (A. Milne-Edwards, 1881)	Gulf of Mexico	HBG914A	KP076006	KP075867	KP076211	KP075854	KP075693	KP076058	N/A
S. debilis (A. Milne-Edwards, 1881)	Gulf of Mexico	HBG551	KP076004	KP075865	N/A	KP075852	KP075695	KP076079	N/A
S. debilis (A. Milne-Edwards, 1881)	Gulf of Mexico	KC4576OPL	KP076005	KP075866	N/A	KP075846	KP075770	KP076080	N/A
S. pellucida (Filhol, 1884)	Taiwan	NTOU M01852	KP075992	KP075924	KP076147	KP075855	KP075707	KP076063	N/A
S. pellucida (Filhol, 1884)	N/A	HBG398	KP075993	KP075925	N/A	KP075857	KP075708	KP076077	N/A
Family Pandalidae Haworth, 1825									
Heterocarpus[s] A. Milne-Edwards, 1881b									
H. ensifer A. Milne-Edwards, 1881	Gulf of Mexico	HBG830	KP076013	KP075931	KP076145	KP075777	KP075762	KP076140	KP076047
H. ensifer A. Milne-Edwards, 1881	Gulf of Mexico	HBG831	KP076012	KP075929	KP076144	KP075778	KP075761	KP076141	N/A
H. ensifer A. Milne-Edwards, 1881	Gulf of Mexico	HBG890	KP076014	KP075930	KP076146	KP075776	KP075763	KP076139	N/A
Family Pasiphaeidae Dana, 1852									
Glyphus[s] Filhol, 1884									
G. marsupialis Filhol, 1884	Gulf of Mexico	HBG1256A	N/A	N/A	KP076198	KP075774	KP075769	KP076137	N/A
G. marsupialis Filhol, 1884	Gulf of Mexico	HBG1262	N/A	N/A	KP076196	KP075771	KP075768	KP076135	N/A
G. marsupialis Filhol, 1884	Gulf of Mexico	HBG1278	N/A	KP075861	KP076197	KP075775	KP075767	KP076136	KP076049
G. aff. *marsupialis*	Gulf of Mexico	HBG1227	N/A	KP075902	N/A	KP075772	KP075766	KP076138	N/A
Family Penaeidae Rafinesque, 1815									
Funchalia Johnson, 1868									
F. villosa (Bouvier, 1905)	Gulf of Mexico	HBG1235	KP076016	N/A	KP076199	N/A	N/A	KP076143	KP076050

N/A = not available for inclusion in this study.
[s] Genera that possess secretory luminescence only.
[p] Genera that possess both secretory and photophore luminescence.

delineation (forward and reverse) on an Applied Biosystems PRISM 3730xl DNA Analyzer.

2.4. Phylogenetic analyses

Primer sequences were removed and remaining sequences were cleaned and assembled using Sequencher 5.0.1 (GeneCodes, Ann Arbor, MI, USA). Protein-coding sequences (COI, H3, NaK) were visually scanned for indels and stop codons to prevent the inclusion of pseudogenes. All sequences were then compared to genes reported in GenBank using the Basic Local Alignment Search Tool (BLAST) (National Center for Biotechnology Information, NCBI) to check for potential contamination. Sequences were aligned using the Multiple Sequence Alignment Tool (MAFFT) (Katoh and Standley, 2013). Missing data were designated with a "?" for any incomplete sequences. Gblocks was used to select for more conserved blocks of 28S because a portion of the 28S sequences were incomplete and of questionable position homology (Castresana, 2000; Talavera and Castresana, 2007). All sequences were uploaded to GenBank (Benson et al., 2011) (Table 1). For the final analysis, individual gene datasets were concatenated in Mesquite 2.75 (Maddison and Maddison, 2011). We used PartitionFinder (Lanfear et al., 2012) to select the optimal partitioning strategy for our dataset, using an Akaike Information Criterion (AIC) information-theoretic metric.

Trees were generated for each individual gene dataset using randomized accelerated maximum likelihood (RAxML v7.4.2) (Stamatakis et al., 2012, 2008, 2005). A total of 1000 searches were used to generate the best ML tree. The best tree was determined by comparing ML estimates, and bootstrap values were mapped onto the resulting topology. Likelihood estimates followed the General Time Reversible (GTR) model of nucleotide substitution with a gamma distribution. Non-parametric bootstrap estimates (Felsenstein, 1985) were used to assess confidence in the final topology for every individual gene set. Individual gene trees were examined for conflicting topologies and potentially contaminated

sequences. Using the same RAxML GTR model and search parameters, a final ML tree was then generated using the partitioned dataset of all concatenated genes.

A Bayesian analysis (BAY) was conducted in MrBayes v3.2.2 (Ronquist et al., 2012) for the concatenated dataset of all genes, following the same partitioning scheme as was used in our RAxML analysis. A GTR substitution model was used for this analysis. Following the partitioning scheme recommended by our PartitionFinder results, the GTR model for each gene/codon used either a gamma-shaped rate variation across sites with a proportion of invariable sites (GTR + I + G) or a discrete gamma-shaped rate variation (GTR + G). Two independent runs, each consisting of 4 chains, were executed for this analysis. The analyses ran for 10,000,000 generations, sampled every 1000 generations, and with a relative burn-in frequency of 25%. A 1% split frequency was reached after about 8.8 million generations, and a 75% majority-rule consensus tree was obtained from the remaining trees. The posterior probability (PP) for each clade was calculated and compared between individual analyses before the combined PP was added to the final BAY tree. All ML and Bay analyses were performed on the High Performance Computing Cluster (Panther) at Florida International University, Miami, FL.

2.5. Character evolution

Ancestral state reconstruction (ASR) was used to trace bioluminescent characters across our Bayesian consensus topology. This method employs statistical approaches to examine character evolution across a given phylogeny (Pagel, 1999). We focused on a single character of bioluminescence that was defined in one of three ways for each species: no bioluminescence (0), secretory bioluminescence only (1), or both secretory and photophore luminescence (2). As there has been some debate between using maximum-likelihood vs. maximum parsimony methods (Cunningham et al., 1998; Royer-Carenzi et al., 2013), we executed both and compared the resulting reconstructions. While maximum parsimony aims to explain character evolution using the fewest possible character changes over time, maximum-likelihood reconstructions take into account all possible character state reconstructions at each node by making use of branch lengths, possible rates of character evolution, and the propagation of character states across terminal taxa (Cunningham et al., 1998; Pagel, 1999). Maximum parsimony has been criticized for underestimating rates of evolutionary change because it fails to consider branch lengths (Crisp and Cook, 2005; Fitch and Beintema, 1990; Fitch and Bruschi, 1987; Huelsenbeck and Lander, 2003). It has been suggested that increased taxon sampling increases accuracy of reconstructions, particularly maximum parsimony methods (Heath et al., 2008; Salisbury and Kim, 2001). However, other studies have shown that more taxa do not necessarily provide a more accurate ASR and have warned against sampling biases (Heath et al., 2008; Li et al., 2010, 2008). We performed multiple reconstruction analyses and found that, regardless of altering taxa numbers and sampling, the results remained unaffected. Both maximum likelihood and maximum parsimony methods were implemented in Mesquite 2.75 (Maddison and Maddison, 2011).

2.6. Transcriptomics

Total RNA was extracted from the eyes of two oplophorid shrimp (*S. debilis* and *O. gracilirostris*) and one benthesicymid shrimp (*B. barletti*) (see Supplementary Table S2) using a NucleoSpin RNA kit following the manufacturer's instructions. Approximately 1 μg of full-length mRNA was reverse transcribed into cDNA using the Clonetech SMARTer kit and protocol. Samples were purified following the protocol detailed in Bybee et al. (2012). Emulsification PCR of the cDNA was carried out using the GS FLX Titanium General Library Preparation Method Manual. Pyrosequencing on a Roche 454 platform was conducted at the DNA Sequencing Center at Brigham Young University, Provo, UT.

The resulting raw transcriptome data were stringently quality checked and 454 pyrosequencing adapters and low-quality sequences (limit = 0.05) were removed. In addition, sequences with ambiguities of more than two consecutive nucleotides were trimmed and any sequences with less than 15 nucleotide bases were removed to maximize assembly efficiency and accuracy. *De novo* transcriptome assembly was subsequently performed using a DeBruijn graph algorithm with the use of CLC Genomics Workbench 7 (CLC Inc., Aarhus, Denmark). Given the coverage and long-read nature of 454 pyrosequencing data (Vera et al., 2008), a minimum contig length of 200 bases and word (kmer) size of 20 were chosen for all assemblies – with bubble sizes depending on average read length of the trimmed sequencing reads for each tissue investigated (*S. debilis* eyes = 399, *O. gracilirostris* eyes = 394, *B. barletti* eyes = 406). Because of the read coverage that 454 pyrosequencing provides as well as the conservative parameters used to avoid contamination and false transcripts, it is possible that some transcripts might not be present in our final assembly. Nevertheless, further analyses confirm the presence of visual genes of interest.

Identification of putative opsin transcripts was achieved by running the concatenated transcriptome assemblies through the Phylogenetically-Informed Annotation (PIA) tool (Speiser et al., 2014), using a MAFFT-profile alignment with a conservative *E*-value cut-off of e^{-4}. This tool identifies protein transcripts involved in vision and light detection from *de novo* transcriptome assemblies in a computationally efficient manner by aligning and objectively placing sequences on pre-calculated phylogenetic trees (Speiser et al., 2014). Previously characterized arthropod opsin protein sequences ($n = 108$) together with outgroup sequences ($n = 16$) spanning a diverse array of taxa ($n = 47$) (Porter et al., 2013) were retrieved from NCBI's GenBank (see Supplementary Table S2). These sequences were combined with our oplophorid and benthesicymid putative opsin sequences, and were aligned using the Multiple Sequence Alignment Tool (MAFFT) (Katoh and Standley, 2013). Missing data were designated with a "?" for any incomplete sequences using Mesquite 2.75 (Maddison and Maddison, 2011).

A phylogram was generated using randomized accelerated maximum likelihood (RAxML v7.4.2) (Stamatakis et al., 2012, 2008, 2005). Likelihood estimates followed the Gamma model of rate heterogeneity. The best tree was determined by comparing ML estimates from a total of 1000 searches, and bootstrap values were mapped onto the resulting topology. Non-parametric bootstrap estimates (Felsenstein, 1985) were used to assess confidence in the final topology. The final ML tree was rooted to a crustacean arthropsin, chordate melanopsins, and opsins from molluscs, platyhelminthes, annelids, and echinoderms. Our definition of opsin photosensitivities as short-wavelength-sensitive, SWS (shorter than 490 nm, UV to blue), and long-wavelength-sensitive, LWS (longer than 490 nm, blue-green to red) was based on sensitivity characteristics determined by previous arthropod opsin studies whose definitions corresponded to evolutionary clades of opsin sequences (Briscoe and Chittka, 2001; Kitamoto et al., 1998; Porter et al., 2009, 2007, 2013). In the past, there have been inconsistencies regarding the classification of UV-sensitive opsins. Various studies have placed UV-sensitive opsins within their own classification (Henze et al., 2012; Porter et al., 2007), while others have defined SWS as encompassing UV-sensitive opsins (Kitamoto et al., 1998; Porter et al., 2009, 2013). We have chosen to follow the latter classification scheme, as it has been shown in some arthropods that a single amino acid polymorphism (lysine vs.

asparagine/glutamate) is one of the mechanisms responsible for the wavelength sensitivity difference between UV- and blue-sensitive opsins (Kashiyama et al., 2009; Salcedo et al., 2003). Additionally, it has been suggested that these opsins share a recent common ancestor (Salcedo et al., 1999). We compared aligned opsin sequences with a *Bos taurus* bovine rhodopsin sequence (accession NM_001014890.1) in order to determine the presence of lysine at amino acid site 90, which would be one indicator of UV-sensitivity (Salcedo et al., 1999). The ML phylogram was used to confirm opsin identity and to characterize the putative oplophorid eye opsin sequences identified by PIA in the preceding analyses.

3. Results

3.1. Phylogenetic relationships

A total of 82 individuals belonging to 30 species from nine genera of Oplophoridae (90% genera coverage) and 11 individuals belonging to seven species across Benthesicymidae, Penaeidae, Pasiphaeidae, Pandalidae, and Nematocarinidae (outgroups) were represented in these analyses. We successfully obtained a total of 86 12S sequences (385 aligned nucleotide positions including gaps), 76 16S sequences (559 characters), 69 COI sequences (659 characters), 88 18S sequences (1883 characters), 87 28S sequences after GBlocks (1837 characters), 92 H3 sequences (328 characters), and 31 NaK sequences (632 characters). The entirety of the dataset is comprised of novel data (529 total sequences and 6283 total characters). A small number of individuals are missing certain sequences due to difficulties during PCR amplification and DNA sequencing. Any missing data were designated with a "?" in the final alignment. Results from PartitionFinder recommended a 13-partition scheme by gene and codon (H3, COI, NaK), which was used in the final analyses. A GTR + I + G evolution model was recommended for 12S, 16S, 18S, 28S, two codon partitions of COI, one codon partition of H3, and two codon partitions of NaK. All other partition subsets used a GTR + G model of evolution. Before outgroup taxa were selected, multiple individuals from nearly all families within Caridea were included in this analysis, which confirmed the monophyly of the family. To preserve the integrity of our alignment, many of these outgroups were removed for the final phylogeny. Additionally, ongoing analyses across Caridea (five genes) and Decapoda (nine genes) have verified this result (Bracken et al., per. communication).

The final maximum likelihood (ML) tree (not shown) is nearly identical to that of the final Bayesian (BAY) tree, with the exception of a few nodes. For instance, the BAY topology shows *Hymenodora* branching earlier when compared to *Ephyrina*, whereas the ML topology shows *Ephyrina* branching earlier. A few conflicting species divergences also occur within the clades of *Oplophorus* and *Meningodora.* Because these differences in topology are minor, only the BAY tree is shown (Fig. 2). Bootstrap values (BP) from the ML tree are added to the posterior probability (PP) values on the BAY tree (Fig. 2). Posterior probabilities are displayed as a percentage (out of 100) to directly aid in support value comparisons. Locality information has been added to each individual.

Both ML and BAY trees support the monophyly of Oplophoridae (PP = 100, BP = 95) (Fig. 2). Our results show a clear split within Oplophoridae into two major clades: a clade containing the genera that exhibit secretory and photophore luminescence (*Oplophorus*, *Janicella*, *Systellaspis* = Clade 1), and a clade containing the genera that exhibit only secretory luminescence (*Hymenodora*, *Ephyrina*, *Meningodora*, *Notostomus*, *Heterogenys*, *Acanthephyra* = Clade 2). The BAY phylogram (Fig. 2) shows significant support (PP > 95 and/or BP > 75) for nearly all genus-level and species-level relationships. There is strong support for the monophyly (PP > 99) of *Oplophorus*, *Janicella*, *Hymenodora*, *Ephyrina*, and *Acanthephyra*. Our analyses provide evidence that *Systellaspis* is polyphyletic, with *Oplophorus* and *Janicella* nested within the genus. *Meningodora* is shown to be paraphyletic in the BAY tree, with *M. vesca* grouping with *Notostomus* albeit with low support (PP = 67). The ML tree, on the other hand, supports the monophyly of *Meningodora*, though this relationship is also not well supported (BP = 55). Additionally, our data suggests possible cryptic speciation between different populations of *J. spinicauda* (Taiwan vs. Gulf of Mexico), *M. mollis* (Taiwan vs. Spain), and *A. pelagica* (Gulf of Mexico vs. North Atlantic). The branch lengths between these same species of different populations are comparable to branch lengths between separate species within Oplophoridae (Fig. 2).

ML trees for individual genes (not shown) were examined for congruence of topologies. Though there were variable levels of resolution, the overall topologies were similar between individual trees and the final ML and BAY trees produced from concatenated datasets. Genus- and species-level relationships were well resolved in 12S, 16S, 28S, COI, H3, and NaK gene trees. The 18S gene tree was unable to resolve genus-level relationships, though this was not surprising as the 18S gene is highly conserved (Hillis and Dixon, 1991).

3.2. Evolution of bioluminescence

A single character, bioluminescence ($n = 3$), was included in the morphological matrix and used for ancestral state reconstruction (ASR). This was defined for each species as completely lacking any form of bioluminescence (0), exhibiting secretory luminescence only (1), or exhibiting both secretory and photophore luminescence (2). We optimized the bioluminescence character across our BAY tree, producing both a maximum likelihood and a maximum parsimony ASR (Fig. 3). Because we did not find that taxon sampling density altered our results, we have chosen to present the reconstructions with the greatest number of taxon representatives. Outgroup representatives and species duplicates were included in the analyses, but are not shown in Fig. 3. The reconstruction from both the likelihood and parsimony analyses support that within oplophorid shrimp, secretory luminescence is ancestral with evidence suggesting it was present in the most recent common ancestor of extant oplophorid shrimp. The maximum likelihood ASR provides a high probability (0.81) that photophore luminescence evolved once within Oplophoridae and is unique to Clade 1, though it is lost in one member of Clade 1, *S. braueri braueri*. The reconstruction from the maximum parsimony analysis was unable to fully resolve the evolution of photophore luminescence, and found that secretory and photophore luminescence are equally probable as the ancestral state for Clade 1. This result does not contradict our ML analysis as maximum parsimony methods have a disadvantage to maximum likelihood in that parsimony methods cannot calculate probabilities of alternative states (Crisp and Cook, 2005).

3.3. Vision and visual systems

Our final RNA-seq dataset was composed of eye transcripts from *B. bartletti* (6511 total contigs, average length = 681 bases, N50 = 741), *O. gracilirostris* (9882 contigs, average length = 605, N50 = 645), and *S. debilis* (13,240 contigs, average length = 620, N50 = 667). Using the Phylogenetically-Informed Annotation (PIA), we identified three potential opsin sequences from *O. gracilirostris* (contig 27, contig 38, contig 1790), three from *S. debilis* (contig 55, contig 665, contig 3453), and two from *B. bartletti* (contig 11, contig 12). A total of 108 previously characterized arthropod opsins spanning 47 taxa and 16 outgroup sequences were added to our 8 shrimp opsin sequences to generate a ML phylogram (Fig. 4). Our phylogenetic analysis shows a separation of SWS and LWS opsins, which is illustrated by the colored vertical bars.

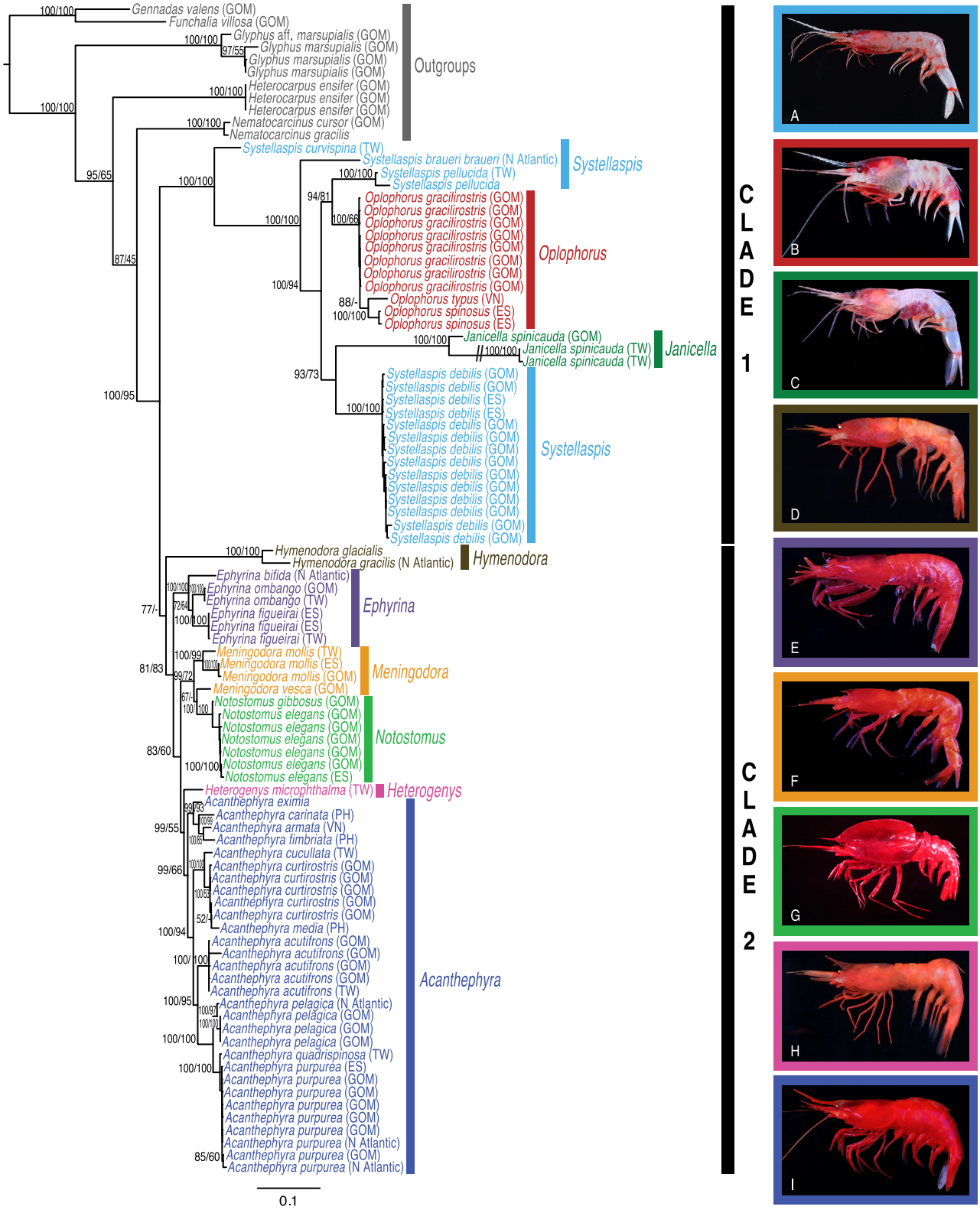

Fig. 2. Bayesian (Bay) phylogram of the family Oplophoridae ($n = 82$) and selected outgroups ($n = 11$) based on a concatenated dataset of 12S (rDNA), 16S (rDNA), COI (protein-coding), 18S (rDNA), 28S (rDNA), H3 (protein-coding), and NaK (protein-coding) gene sequences. BAY posterior probabilities and ML bootstrap values are displayed above branches (BAY/ML). The colored vertical bars indicate genera or outgroups. Locality information includes the Gulf of Mexico (GOM), the North Atlantic Ocean near the Mid-Atlantic Ridge between the Azores and Iceland (N Atlantic), Spain (ES), the Philippines (PH), Vietnam (VN) and Taiwan (TW). Photographs of a few representatives including *Systellaspis pellucida* (A), *Oplophorus gracilirostris* (B), *Janicella spinicauda* (C), *Hymenodora gracilis* (D), *Ephyrina ombango* (E), *Meningodora mollis* (F), *Notostomus gibbosus* (G), *Heterogenys microphthalma* (H), and *Acanthephyra armata* (I) are included. Photographs by Tin-Yam Chan.

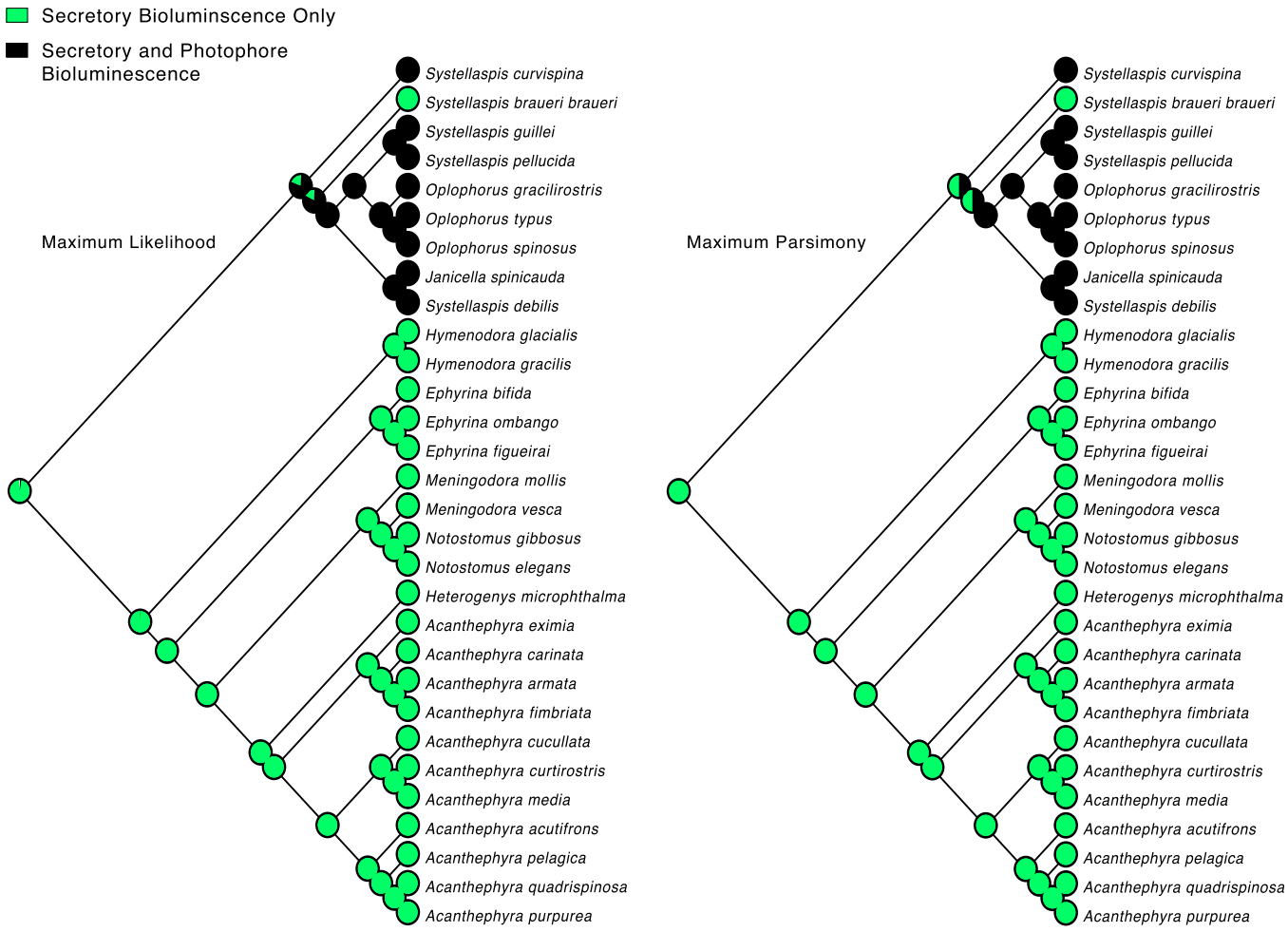

Fig. 3. Ancestral state reconstruction depicting the character evolution of secretory and photophore bioluminescence. The analyses used maximum likelihood (left) and maximum parsimony (right) optimized across the Bayesian cladogram.

Our analysis supports that two eye opsins from *B. bartletti* (contig 11, contig 12), one from *S. debilis* (contig 55), and two from *O. gracilirostris* (contig 38, contig 27) are nested within LWS opsins. There are two opsins from *S. debilis* (contig 3453 and contig 665) and one from *O. gracilirostris* (contig 1790) that are nested within SWS opsins. Of these, one *S. debilis* and one *O. gracilirostris* opsin sequence (contig 665 and contig 1790) fall within proximity of the clade containing previously characterized near-UV-sensitive opsins. Although these two contigs do not contain a lysine at bovine amino acid site 90, they both show intriguing substitution patterns in sites of possible influence to spectral tuning (Katti et al., 2010; Takahashi and Ebrey, 2003), while maintaining conserved features characteristic of arthropod rhabdomeral opsins (Katti et al., 2010; Porter et al., 2007). UV-sensitivity can arise through a variety of opsin modifications (Devine et al., 2013), and the observed amino acid modifications could putatively confer *S. debilis* and *O. gracilirostris* the near-UV sensitivity previously described in the literature (Cronin and Frank, 1996; Frank and Case, 1988; Kent, 1997). *Benthesicymus bartletti* eye opsins are not found nested with any SWS opsins.

4. Discussion

4.1. Evolutionary relationships

Phylogenetic analyses are very effective for tracing character evolution and in this case, modes of bioluminescence in oplophorid shrimp. Unfortunately, few studies have attempted to characterize the evolutionary relationships and systematic arrangements of the oplophorid genera and the phylogeny has remained in flux. A study by Bracken et al. (2009) included only seven oplophorid individuals spanning six different species and only four genera. A study by Chan et al. (2010) included ten oplophorid individuals spanning ten different species and nine genera. The molecular evidence used for phylogenetic reconstructions by both of these studies only included 18S nuclear and 16S mitochondrial genes. Though effective, particularly at and above the family level, 18S has been found to provide relatively low divergence between species (Chu et al., 2009). Furthermore, 18S has been shown to evolve very slowly and therefore be highly conserved across taxa (Chu et al., 2009; Hillis and Dixon, 1991). Our study presents the most comprehensive phylogenic analyses of Oplophoridae to date, incorporating molecular data from seven different genes, and across 82 oplophorid individuals spanning 30 unique species and 90% genera coverage. With the exception of a few nodes, there is strong support for most branches in our BAY topology.

Bracken et al. (2009) suggested that Oplophoridae might be polyphyletic, as there was no statistical support of *Systellaspis* grouping with *Ephyrina*, *Acanthephyra*, and *Meningodora*. Chan et al. (2010) recommended that Oplophoridae be split into two families: Oplophoridae that contains *Systellaspis*, *Oplophorus*, and *Janicella*; and resurrecting Acanthephyridae Bate, 1888 that contains *Acanthephyra*, *Ephyrina*, *Meningodora*, *Kemphyra*,

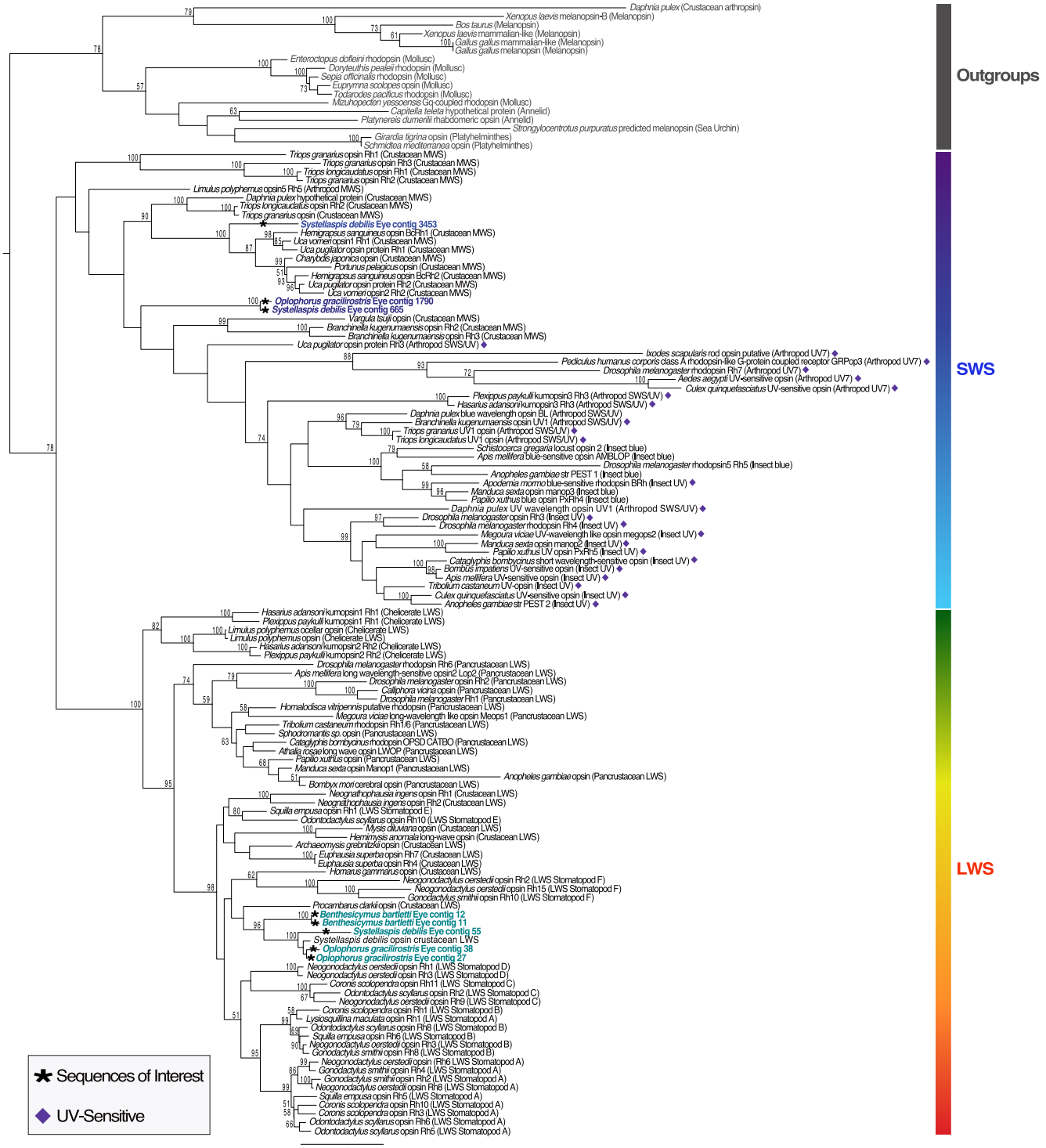

Fig. 4. Maximum likelihood (RAxML) phylogram of opsin visual proteins in arthropods, including *Systellaspis debilis*, *Oplophorus gracilirostris*, and *Benthesicymus bartletti* transcriptome contigs from the eyes (in bold font and branches marked with a black star). Arthropsin, melanopsin, and mollusc, platyhelminthes, annelid, and echinoderm opsin sequences were used as outgroups. Descriptions of visual genes, determined by phylogenetic placement in Porter et al. (2013), are included in parenthesis. Bootstrap values greater than or equal to 50% are displayed above branches. The colored vertical bars represent two definitions of spectral sensitivities: short-wavelength-sensitive, SWS (shorter than 490 nm, UV to blue) and long-wavelength-sensitive (greater than 490 nm, blue-green to red). UV-sensitive opsins are designated with a purple diamond. (For interpretation of the references to color in this figure legend, the reader is referred to the web version of this article.)

Heterogenys, *Hymenodora*, and *Notostomus*. In contrast, our analyses support the monophyletic status of Oplophoridae, along with studies across Caridea and Decapoda, which are currently ongoing and will verify this result (Bracken-Grissom et al., per. communication). There are two distinct clades within the Oplophoridae phylogeny: Clade 1, which exhibits both secretory and photophore luminescence and Clade 2, which exhibits only secretory luminescence. The genera within Clade 2 have, along with *Kemphyra*, been recently grouped within the resurrected family Acanthephyridae Bate, 1888 (Chan et al., 2010; De Grave and Fransen, 2011). In addition to the photophore-bearing characteristic, Clade 1 species tend to have larger eyes, which

are often associated with species that inhabit shallower depths, than most Clade 2 species (Chan et al., 2010).

Our analyses, which include 4 of the 9 species of *Systellaspis* (De Grave and Fransen, 2011), strongly support that *Systellaspis* is polyphyletic with *Oplophorus* and *Janicella* nesting in between *Systellaspis* (Fig. 2). Interestingly, *J. spinicauda* has been described as a morphological intermediate between *Oplophorus* and *Systellaspis* (Chace, 1986; Chan et al., 2010). *Systellaspis* is a species-rich genus and there are a large number of discrepancies in morphology among some species (see Chace, 1986). Future studies that include greater species coverage of *Systellaspis* will need to be conducted to verify that this genus is polyphyletic and to determine how the genus should be subdivided, particularly because the type-species *S. lanceocaudata* Spence Bate, 1888 is not included in this work.

There may be cryptic speciation between different populations of *Janicella spinicauda*, *Meningodora mollis*, and *Acanthephyra pelagica*, which are supported by our BAY phylogram (Fig. 2). In these cases, the branch lengths between the same species from different populations are comparable to the branch lengths found between different species within Oplophoridae. This analysis included three specimens of *J. spinicauda* (two from the Taiwan and one from the Gulf of Mexico), three specimens of *M. mollis* (one each from Spain, the Gulf of Mexico, and Taiwan), and four specimens of *A. pelagica* (three from the Gulf of Mexico and one from the North Atlantic between the Azores and Iceland). We recommend additional sampling and analyses of these species to confirm this result.

4.2. Evolution of bioluminescence

Our ancestral state reconstruction supports a single origin of evolution for secretory luminescence within Oplophoridae. It has been shown that this defensive mechanism evolved due to predatory pressures within the light-limited environments that all oplophorid shrimp inhabit (Bauer, 2004; Haddock et al., 2010) (Fig. 1). Though many species are strong vertical migrators and routinely ascend into shallow waters at night, all oplophorid shrimps have daytime depths below 200 m and are considered meso- and/or bathypelagic (Chace, 1986; Chan et al., 2010). Bioluminescent defense mechanisms designed to startle or blind predators are not uncommon in the deep sea, and have been witnessed in organisms outside of Crustacea, including fish, squid, and jellyfish (Widder, 2002). It has been shown that oplophorid secretory luminescence is related to homogenates produced in the hepatopancreas (Herring, 1976, 1985) and substrates found in stomach tissues (Shimomura et al., 1980; Thomson et al., 1995).

Our analysis supports that the emergence of photophores occurred later in the evolution of Oplophoridae and was restricted to Clade 1. Photophores can be found along the length of the body, including the eyes, limbs, cephalothorax and abdomen (Herring, 2007; Nowel et al., 1998). They are concentrated primarily on the ventral surface, where they would aid most in counter-illumination (Nowel et al., 1998). Clade 2 tends to inhabit deeper waters (~500–1200 m), while Clade 1 commonly inhabits shallower waters (~490–900 m) during the daytime and migrates to even shallower waters (~30–375 m) at night (Chan et al., 2010; Frank and Widder, 1994a, 1996) to feed.

Photophore luminescence may have evolved in species that tend to inhabit shallower waters, where downwelling light from the surface would be more prominent in the water column and where counter-illumination camouflage would be useful against potential predators. It has been reported that shallower species, such as *S. debilis*, bear many photophores, while *S. braueri braueri*, which is found between 500 and 2000 m (Krygier and Pearcy, 1981), completely lacks photophores (Herring, 1985). Furthermore, juvenile *S. cristata*, which inhabit shallower waters, have more prominent photophores than their adult counterparts who generally live in deeper waters (Herring, 1985). This supports the hypothesis that the presence of photophores in oplophorid shrimp has a direct relationship to depth distribution. However, Clade 1 genera are not the only oplophorid shrimp that exhibit diurnal vertical migration. All but four to six species of *Acanthephyra* vertically migrate, and one species, *A. quadrispinosa*, has been found in waters as shallow as 27 m during nighttime (Chace, 1986). Despite these vertical migration patterns, no species of *Acanthephyra* have been reported to possess photophores (Frank and Case, 1988; Herring, 1985; Welsh and Chace, 1937).

4.3. Adaptation of visual systems

In the deep sea, the only forms of light are downwelling blue light from the surface (~475 nm) (Cronin, 1986; Dartnall, 1975; Jerlov, 1968) and bioluminescence, most commonly peaking in the blue spectrum (between 460 and 490 nm) (Herring, 1983; Latz et al., 1988; Widder et al., 1983). It is therefore probable to expect that the visual sensitivity of organisms in this environment would be limited to blue light wavelengths (Frank and Widder, 1996). Indeed, most deep-sea species are found to possess a singular visual pigment that absorbs maximally in the blue-green spectrum (468–540 nm) (Warrant and Locket, 2004). However, a near-ultraviolet (390–410 nm) photopigment has been found in *Systellaspis*, *Oplophorus*, and *Janicella* (Cronin and Frank, 1996; Frank and Case, 1988; Kent, 1997). These Clade 1 oplophorids have been shown to possess two photopigments (one sensitive to blue-green and one sensitive to near-UV light), while Clade 2 oplophorids bear only a single photopigment (sensitive to blue-green light) (Cronin and Frank, 1996; Frank and Case, 1988; Frank and Widder, 1994a,b; Gaten et al., 2004; Herring, 1996). Spectral sensitivities of oplophorid shrimp, in species both with and without photophores, have been measured using microspectrophotometry, electroretinograms, behavioral responses (changes in pleopod beating rate, tilt, and flex of the body), and morphology (Cronin and Frank, 1996; Frank and Case, 1988; Frank and Widder, 1994a,b; Gaten et al., 2004; Kent, 1997). However, there have been no genetic analyses conducted to attempt to characterize the visual genes controlling this light detection. In this study, we focused on opsin proteins due to their significance in light perception. Visual pigments absorb photons of light and, through a resulting phototransduction cascade, convert this light into an electrical signal that leads to vision (Kashiyama et al., 2009; Nathans, 1987). An opsin protein, along with a chromophore, is the primary component of any visual pigment (Kashiyama et al., 2009; Porter et al., 2011; Wald, 1968) and is therefore essential for light detection. Opsins are responsible for tuning spectral sensitivity and it has been shown that altering an opsin amino acid sequence can alter the wavelengths to which visual pigments are sensitive (Carleton and Kocher, 2001).

We found several opsin sequences within our RNA-seq data and characterized them by implementing a phylogenetic analysis with previously characterized opsin sequences. There is, however, the potential that some transcripts may be missing from our final assembly due to the read coverage of 454 pyrosequencing as well as the stringent parameters used to prevent contamination and false transcripts. Our findings suggest that *B. barletti* has only LWS eye opsins that form visual pigments sensitive to wavelengths greater than 490 nm (Fig. 4). This falls within the blue-green visual spectra expected for deep-sea-dwelling organisms. The eyes of *S. debilis* and *O. gracilirostris* were also found to contain LWS opsins, which is in accordance with the results of previous studies that found that the photosensitivity of these oplophorid species had a sensitivity maximum to blue-green wavelengths (about 490–510 nm) (Frank and Case, 1988; Frank and Widder, 1994a, 1996; Gaten et al., 2004). *Systellaspis debilis* and *O. gracilirostris* also possess SWS eye opsins, at least two of which (contig 665 and contig

1790) present amino acid substitutions in sites known to influence spectral tuning in other species (Katti et al., 2010; Takahashi and Ebrey, 2003). Given that UV-sensitivity can be conferred by different mechanisms and opsin modifications (Devine et al., 2013) the observed amino acid modifications and the position of these opsins in the phylogram suggest they could be involved in near-UV sensitivity. This finding aligns with previous physiological and behavioral studies (Frank and Case, 1988; Frank and Widder, 1994a, 1996), which demonstrated the presence of near-UV sensitivity maxima (390–410 nm) in the eyes of photophore-bearing oplophorids. These previous studies, together with the structural studies of Gaten et al. (2004), also confirmed the presence of an eighth rhabdomere, which has been linked to the occurrence of a UV visual pigment in the eyes of shallow water crustaceans.

It has been suggested that Clade 1 shrimp might be able to use spectral characteristics of downwelling UV light to determine their depth as well as the time of day, thereby cueing their vertical migrations (Frank and Case, 1988). This has since been proven to not be the case because, although UV light may be present at depths up to 600 m, the change in spectral shape that occurs with depth and time of day is not great enough to be detected below 150 m (Frank and Widder, 1996). The triggering mechanism that cues upward migrations of the photophore-bearing oplophorids, or other vertical migrators with UV sensitivity remains unknown.

Photophores emit light at a slightly different wavelength and more importantly, have a much narrower spectral bandwidth than that of secretory luminescence (Herring, 1983; Latz et al., 1988). It has been suggested that the dual visual-pigment system allows Clade 1 oplophorid shrimp to distinguish between these modes of bioluminescence (Frank and Case, 1988; Gaten et al., 2004). Light of different bandwidths and wavelengths can have varying stimulatory effects on a given photoreceptor, and the mismatch and combination of more than one visual pigment may allow the shrimp to discriminate between different spectral characteristics (Cronin and Frank, 1996; Gaten et al., 2004). Another proposal is that the dual visual-pigment system allows for heightened contrast detection to enhance differentiation between radiance characteristics of the carapace or secretory luminescence and that of background light (Gaten et al., 2004). Gaten et al. (2004) proposed that the deeper-living oplophorid genera have abandoned a dual system in favor of a single visual-pigment system, which may allow for increased light sensitivity in deeper waters where light is more limited (Lythgoe, 1979).

It has also been suggested that the shrimp are able to use their dual visual-pigment system to improve detection of the surrounding downwelling light and more closely match their photophore luminescence for counter-illumination (Frank and Widder, 1996). It has been argued that, in order for this to be the case, rhabdoms in the dorsal part of the eye would need to be structurally modified as this is the part of the eye that would be used to detect downwelling light (Gaten et al., 2004). Gaten et al. (2004), however, showed that modifications were only present in the ventral part of the eye and concluded it was unlikely that dual visual-pigment systems are used for photophore emission matching. Research is ongoing to investigate the precise method in which these shrimps are able to so accurately match their photophore luminescence with the downwelling irradiance.

To date, numerous explanations have been proposed to explain the purpose and evolutionary significance of a dual visual-pigment system in photophore-bearing oplophorid shrimp. Even though the definite answers to these questions remain elusive, advances in novel molecular techniques may provide the key to fully comprehending the evolution of light detection in the deep sea. This study represents the first molecular approach to understanding oplophorid vision and presents the first examination of visual genes within the family Oplophoridae, specifically those controlling opsin proteins. We advocate the continuation of transcriptomic studies to gain further insight into the bioluminescent and light-detecting capabilities of these shrimps and other fascinating deep-sea organisms.

Acknowledgments

We thank the EAGER award (IOS – 1045243), the Decapod AToL (DEB – 0531762), and the Ministry of Science and Technology, Taiwan, R.O.C. for financial support of this study. We thank Darryl L. Felder at the University of Louisiana at Lafayette, Keith A. Crandall at George Washington University, and José María Landeira at the University of La Laguna for providing many samples for these molecular analyses. We thank Seth Bybee at Brigham Young University and Shaina Lear, Laura Timm, and Adriana Suarez at Florida International University for their assistance with laboratory work. We also thank Todd Oakley, Daniel Speiser, and Sabrina Pankey at the University of California, Santa Barbara and Megan Porter at the University of South Dakota for their advice and input into the preparation of this manuscript. We have no conflict of interest to declare.

Appendix A. Supplementary material

Supplementary data associated with this article can be found, in the online version, at http://dx.doi.org/10.1016/j.ympev.2014.11.013.

References

Apakupakul, K., Siddall, M.E., Burreson, E.M., 1999. Higher level relationships of leeches (Annelida: Clitellata: Euhirudinea) based on morphology and gene sequences. Mol. Phylogenet. Evol. 12, 350–359.

Bauer, R.T., 2004. Remarkable Shrimps: Adaptations and Natural History of the Carideans. The University of Oklahoma Press, Publishing Division of the University, Norman.

Benson, D.A., Karsch-Mizrachi, I., Clark, K., Lipman, D.J., Ostell, J., Sayers, E.W., 2011. GenBank. Nucl. Acids Res., 1–6.

Bracken, H., Toon, A., Felder, D.L., Martin, J.W., Finley, M., Rasmussen, J., Palero, F., Crandall, K.A., 2009. The decapod tree of life: compiling the data and moving toward a consensus of decapod evolution. Arthropod Syst. Phylogenet. 67, 99–116.

Bracken-Grissom, H., Ettinger, M., Cabezas, P., Feldmann, R., Schweitzer, C., Ahyong, S.T., Felder, D.L., Lemaitre, R., Crandall, K.A., 2013. A comprehensive and integrative approach to reconstruct the evolutionary history of the Anomura (Crustacea: Decapoda). BMC Evol. Biol. 13, 128.

Bracken-Grissom, H.D., Ahyong, S.T., Wilkinson, R.D., Feldman, R.M., Schweitzer, C.E., Breinholt, J.W., Bendall, M., Palero, F., Chan, T.Y., Felder, D.L., Robles, R., Chu, K.H., Tsang, L.M., Kim, D., Martin, J.W., Crandall, K.A., 2014. The emergence of lobsters: phylogenetic relationships, morphological evolution and divergence time comparisons of an ancient group (Decapoda: Achelata, Astacidea, Glypheidea, Polychelida). Syst. Biol. 63, 457–479.

Briscoe, A.D., Chittka, L., 2001. The evolution of color vision in insects. Annu. Rev. Entomol. 46.

Buhay, J.E., Moni, G., Mann, N., Crandall, K.A., 2007. Molecular taxonomy in the dark: evolutionary history, phylogeography, and diversity of cave crayfish in the subgenus *Aviticambarus*, genus *Cambarus*. Mol. Phylogenet. Evol. 42, 435–448.

Bybee, S.M., Johnson, K.K., Gering, E.J., Whiting, M.F., Crandall, K.A., 2012. All the better to see you with: a review of odonate color vision with transcriptomic insight into the odonate eye. Organ. Diversity Evol. 12, 241–250.

Carleton, K.L., Kocher, T.D., 2001. Cone opsin genes of African cichlid fishes: tuning spectral sensitivity by differential gene expression. Mol. Biol. Evol. 18, 1540–1550.

Castresana, J., 2000. Selection of conserved blocks from multiple alignments for their use in phylogenetic analysis. Mol. Biol. Evol. 17, 540–552.

Chace Jr., F.A., 1986. The Caridean shrimps (Crustacea: Decapoda) of the Albatross Philippine Expedition, 1907–1910, Part 4: Families Oplophoridae and Nematocarcinidae. Smithson. Contrib. Zool. 432, 1–82.

Chan, T.Y., Lei, H.C., Li, C.P., Chu, K.H., 2010. Phylogenetic analysis using rDNA reveals polyphyly of Oplophoridae (Decapoda: Caridea). Invertebr. Syst. 24, 172–181.

Chu, K.H., Tsang, L.M., Ma, K.Y., Chan, T.Y., Ng, P.K.L., 2009. Decapod phylogeny: what can protein-coding genes tell us? In: Martin, J.W., Crandall, K.A., Felder, D.L. (Eds.), Decapod Crustacean Phylogenetics. CRC Press, Taylor & Francis Group.

Colgan, D.J., McLauchlan, A., Wilson, G.D.F., Livingston, S.P., Edgecombe, G.D., Macaranas, J., Cassis, G., Gray, M.R., 1998. Histone 3 and U2 snRNA DNA sequences and arthropod molecular evolution. Aust. J. Zool. 46, 419–437.
Crandall, K.A., Fitzpatrick, J.F., 1996. Crayfish molecular systematics: using a combination of procedures to estimate phylogeny. Syst. Biol. 45, 1–26.
Crisp, M.D., Cook, L.G., 2005. Do early branching lineages signify ancestral traits? Trends Ecol. Evol. 20, 122–128.
Cronin, T.W., 1986. Photoreception in marine invertebrates. Am. Zool. 26, 403–415.
Cronin, T.W., Frank, T.M., 1996. A short-wavelength photoreceptor class in a deep-sea shrimp. Proc. R. Soc. Lond. B: Biol. Sci. 263, 861–865.
Cunningham, C.W., Omland, K.E., Oakley, T.H., 1998. Reconstructing ancestral character states: a critical reappraisal. Trends Ecol. Evol. 13, 361–366.
Dartnall, H.J.A., 1975. Assessing the fitness of visual pigments for their photic environments. In: Vision in Fishes – New Approaches in Research. Plenum Press, New York, pp. 543–563.
De Grave, S., Fransen, C.H.J.M., 2011. Carideorum catalogus: the recent species of the dendrobranchiate, stenopodidean, procarididean and caridean shrimps (Crustacea: Decapoda). Zool. Meded. (Leiden) 85, 195–589.
De Grave, S., Pentcheff, N.D., Ahyong, S.T., Chan, T.-Y., Crandall, K.A., Dworschak, P.C., Felder, D.L., Feldman, R.M., Fransen, C., Goulding, L., Lemaitre, R., Low, M., Martin, J., Ng, P., Schweitzer, C.E., Tan, S.H., Tsudy, D., Wetzer, R., 2009. A classification of living and fossil genera of decapod crustaceans. Raffles Bull. Zool. 21, 1–109.
Denton, E.J., Gilpin-Brown, J.B., Wright, P.G., 1972. The angular distribution of the light produced by some mesopelagic fish in relation to their camouflage. Proc. R. Lond. B (The Royal Society) 182, 145–158.
Denton, E.J., Herring, P.J., Widder, E.A., Latz, M.F., Case, J.F., 1985. The roles of filters in the photophores of oceanic animals and their relation to vision in the oceanic environment. Proc. R. Lond. B (The Royal Society) 225, 63–97.
Devine, E.L., Oprian, D.D., Theobald, D.L., 2013. Relocating the active-site lysine in rhodopsin and implications for evolution of retinylidene proteins. PNAS 110, 13351–13355.
Felsenstein, J., 1985. Confidence-limits on phylogenies with a molecular clock. Syst. Zool. 34, 152–161.
Fitch, W.M., Beintema, J.J., 1990. Correcting parsimonious trees for unseen nucleotide substitutions: the effect of dense branching as exemplified by ribonuclease. Mol. Biol. Evol. 7, 438–443.
Fitch, W.M., Bruschi, M., 1987. The evolution of prokaryotic ferredoxins – with a general method correcting for unobserved substitutions in less branched lineages. Mol. Biol. Evol. 4, 381–394.
Folmer, O., Black, M., Hoeh, W., Lutz, R., Vrijenhoek, R., 1994. DNA primers for amplification of mitochondrial cytochrome c oxidase subunit I from diverse metazoan invertebrates. Mar. Biotechnol. 3, 294–299.
Frank, T.M., Case, J.F., 1988. Visual spectral sensitivities of bioluminescent deep-sea crustaceans. Biol. Bull. 175, 261–273.
Frank, T.M., Widder, E.A., 1994a. Comparative-study of behavioral sensitivity thresholds to near-UV and blue-green light in deep-sea crustaceans. Mar. Biol. 121, 229–235.
Frank, T.M., Widder, E.A., 1994b. Evidence for behavioral sensitivity to near-UV light in the deep-sea crustacean Systellaspis-debilis. Mar. Biol. 118, 279–284.
Frank, T.M., Widder, E.A., 1996. UV light in the deep-sea: in situ measurements of downwelling irradiance in relation to the visual threshold sensitivity of UV-sensitive crustaceans. Mar. Freshw. Behav. Physiol. 27, 189–197.
Gaten, E., Shelton, P.M.J., Nowel, M.S., 2004. Contrast enhancement through structural variations in the rhabdoms of oplophorid shrimps. Mar. Biol. 145, 499–504.
Gracias, K.S., McKillip, J.L., 2004. A review of conventional detection and enumeration methods for pathogenic bacteria in food. Can. J. Microbiol. 50, 883–890.
Haddock, S.H.D., Moline, M.A., Case, J.F., 2010. Bioluminescence in the sea. Annu. Rev. Mar. Sci. 2, 443–493.
Heath, T.A., Hedtke, S.M., Hillis, D.M., 2008. Taxon sampling and the accuracy of phylogenetic analyses. J. Syst. Evol. 46, 239–257.
Henze, M.J., Dannenhauer, K., Kohler, M., Labhart, T., Gesemann, M., 2012. Opsin evolution and expression in arthropod compound eyes and ocelli: insights from the cricket Gryllus bimaculatus. BMC Evol. Biol. 12.
Herring, P.J., 1976. Bioluminescence in decapod crustacea. J. Mar. Biol. Assoc. UK 56, 1029–1047.
Herring, P.J., 1983. The spectral characteristics of luminous marine organisms. P. Roy. Soc. Lond. B: Biol. Sci. 220, 183–217.
Herring, P.J., 1985. Bioluminescence in the crustacea. J. Crustac. Biol. 5, 557–573.
Herring, P.J., 1996. Light, colour and vision in the ocean. In: Summerhayes, C.P., Thorpe, S.A. (Eds.), Oceanography: An Illustrated Guide. Mason Publishing, London, pp. 212–227.
Herring, P.J., 2007. Sex with the lights on? A review of bioluminescent sexual dimorphism in the sea. J. Mar. Biol. Assoc. UK 87, 829–842.
Hillis, D.M., Dixon, M.T., 1991. Ribosomal DNA: molecular evolution and phylogenetic inference. Quart. Rev. Biol. 66, 411–453.
Huelsenbeck, J.P., Lander, K.M., 2003. Frequent inconsistency of parsimony under a simple model of cladogenesis. Syst. Biol. 52, 641–648.
Jerlov, N.G. (Ed.), 1968. Optical Oceanography. Elsevier Publishing Company, Amsterdam, The Netherlands.
Kashiyama, K., Seki, T., Numata, H., Goto, S.G., 2009. Molecular characterization of visual pigments in Branchiopoda and the evolution of opsins in Arthropoda. Mol. Biol. Evol. 26, 299–311.
Katoh, K., Standley, D.M., 2013. MAFFT multiple sequence alignment software version 7: improvements in performance and usability. Mol. Biol. Evol. 30, 772–780.
Katti, C., Kempler, K., Porter, M.L., Legg, A., Gonzalez, R., Garcia-Rivera, E., Dugger, D., Battelle, B.-A., 2010. Opsin co-expression in Limulus photoreceptors: differential regulation by light and a circadian clock. J. Exp. Biol. 213, 2589–2601.
Kent, J., 1997. The visual pigments of deep-sea crustaceans. PhD Thesis. School of Biological Sciences. University of Bristol, UK.
Kitamoto, J., Sakamoto, K., Ozaki, K., Mishina, Y., Arikawa, K., 1998. Two visual pigments in a single photoreceptor cell: identification and histological localization of three mRNAs encoding visual pigment opsins in the retina of the butterfly Papilio xuthus. J. Exp. Biol. 201, 1255–1261.
Krygier, E.E., Pearcy, W.G., 1981. Vertical distribution and biology of pelagic decapod crustaceans off Oregon. J. Crustac. Biol. 1, 70–95.
Lanfear, R., Calcott, B., Ho, S.Y.W., Guindon, S., 2012. PartitionFinder: combined selection of partitioning schemes and substitution models for phylogenetic analyses. Mol. Biol. Evol. 29, 1695–1701.
Latz, M.I., Frank, T.M., Case, J.F., 1988. Spectral composition of bioluminescence of epipelagic organisms from the Sargasso Sea. Mar. Biol. 98, 441–446.
Li, G., Ma, J., Zhang, L., 2010. Greedy selection of species for ancestral state reconstruction on phylogenies: elimination is better than insertion. PLoS ONE 5.
Li, G., Steel, M., Zhang, L., 2008. More taxa are not necessarily better for the reconstruction of ancestral character states. Syst. Biol. 57, 647–653.
Lythgoe, J.N., 1979. The Ecology of Vision. Oxford University Press, UA.
Ma, K.Y., Chan, T.-Y., Chu, K.H., 2009. Phylogeny of penaeoid shrimps (Decapoda: Penaeoidea) inferred from nuclear protein-coding genes. Mol. Phylogenet. Evol. 53, 45–55.
Maddison, W.P., Maddison, D.R., 2011. Mesquite: A Modular System for Evolutionary Analysis, Version 2.75.
Nathans, J., 1987. Molecular biology of visual pigments. Annu. Rev. Neurosci. 10, 163–194.
Nowel, M.S., Shelton, P.M.J., Herring, P.J., 1998. Cuticular photophores of two decapod crustaceans, Oplophorus spinosus and Systellaspis debilis. Biol. Bull. 195, 290–307.
Pagel, M., 1999. The maximum likelihood approach to reconstructing ancestral character states of discrete characters on phylogenies. Syst. Biol. 48, 612–622.
Palumbi, S., Martin, A., Romano, S., McMillan, W.O., Stice, L., Grabowski, G., 1991. The Simple Fool's Guide to PCR. Department of Zoology and Kewalo Marine Laboratory, University of Hawaii, Honolulu.
Palumbi, S.R., 1996. Nucleic Acids, II: The Polymerase Chain Reaction. Sinauer Associates, Sunderland, Mass.
Porter, M.L., Blasic, J.R., Bok, M.J., Cameron, E.G., Pringle, T., Cronin, T.W., Robinson, P.R., 2011. Shedding new light on opsin evolution. Proc. R. Soc. B: Biol. Sci. 279, 3–14.
Porter, M.L., Bok, M.J., Robinson, P.R., Cronin, T.W., 2009. Molecular diversity of visual pigments in Stomatopoda (Crustacea). Vis. Neurosci. 26, 255–265.
Porter, M.L., Cronin, T.W., McClellan, D.A., Crandall, K.A., 2007. Molecular characterization of crustacean visual pigments and the evolution of pancrustacean opsins. Mol. Biol. Evol. 24, 253–268.
Porter, M.L., Speiser, D.I., Zaharoff, A.K., Caldwell, R.L., Cronin, T.W., Oakley, T.H., 2013. The evolution of complexity in the visual systems of stomatopods: insights from transcriptomics. Integr. Comp. Biol. 53, 39–49.
Ralser, M., Querfurth, R., Warnatz, H., Lehrach, H., Yaspo, M., Krobitsch, S., 2006. An efficient and economic enhancer mix for PCR. Biochem. Biophys. Res. Commun. 347, 747–751.
Roda, A., Pasini, P., Mairasoli, M., Michelini, E., Guardigli, M., 2004. Biotechnological applications of bioluminescence and chemiluminescence. Trends Biotechnol. 22, 295–303.
Ronquist, F., Teslenko, M., van der Mark, P., Ayres, D.L., Darling, A., Hohna, S., Larget, B., Liu, L., Suchard, M.A., Huelsenbeck, J.P., 2012. MrBayes 3.2: efficient Bayesian phylogenetic inference and model choice across a large model space. Syst. Biol. 61, 539–542.
Royer-Carenzi, M., Pontarotti, P., Didier, G., 2013. Choosing the best ancestral character state reconstruction method. Math. Biosci. 242, 95–109.
Salcedo, E., Huber, A., Henrich, S., Chadwell, L.V., Chou, W., Paulsen, R., Britt, S.G., 1999. Blue- and green-absorbing visual pigments of drosophila: ectopic expression and physiological characterization of the R8 photoreceptor cell-specific Rh5 and Rh6 rhodopsins. J. Neurosci. 19, 10716–10726.
Salcedo, E., Zheng, L., Phistry, M., Bagg, E.E., Britt, S.G., 2003. Molecular basis for ultraviolet vision in invertebrates. J. Neurosci. 23, 10873–10878.
Salisbury, B.A., Kim, J., 2001. Ancestral state estimation and taxon sampling density. Syst. Biol. 50, 557–564.
Schubart, C.D., Cuesta, J.A., Felder, D.L., 2002. Glyptograpsidae, a new brachyuran family from Central America: larval and adult morphology, and a molecular phylogeny of the Grapsoidea. J. Crustac. Biol. 22, 28–44.
Shimomura, O., Inoue, S., Johnson, F.H., Haneda, Y., 1980. Widespread occurrence of coelenterazine in marine bioluminescence. Comp. Biochem. Physiol., B: Comp. Biochem. 65, 435–437.
Speiser, D.I., Pankey, M.S., Zaharoff, A.K., Batelle, B.A., Bracken-Grissom, H.D., Brienholt, J.W., Bybee, S., Cronin, T.W., Garm, A., Patel, N.H., Porter, M.L., Protas, M.E., Rivera, A.S., Serb, J.M., Zigler, K.S., Crandall, K.A., Oakley, T.H., 2014. Using phylogenetically-informed annotation (PIA) to search for light-interacting genes in transcriptomes from non-model organisms. BMC Bioinf. 15, 1–12.

Stamatakis, A., Aberer, A.J., Goll, C., Smith, S.A., Berger, S.A., Izquierdo-Carrasco, F., 2012. RAxML-light: a tool for computing terabyte phylogenies. Bioinformatics 28, 2064–2066.
Stamatakis, A., Hoover, P., Rougemont, J., 2008. A rapid bootstrap algorithm for the RAxML web servers. Syst. Biol. 57, 758–771.
Stamatakis, A., Ludwig, T., Meier, H., 2005. RAxML-III: a fast program for maximum likelihood-based inference of large phylogenetic trees. Bioinformatics 21, 456–463.
Steinberg, S.M., Poziomek, E.J., Engelmann, W.H., Rogers, R.K., 1995. A review of environmental applications of bioluminescence measurements. Chemosphere 30, 2155–2197.
Takahashi, Y., Ebrey, T.G., 2003. Molecular basis of spectral tuning in the newt short wavelength sensitive visual pigment. Biochemistry 42, 6025–6034.
Talavera, G., Castresana, J., 2007. Improvement of phylogenies after removing divergent and ambiguously aligned blocks from protein sequence alignments. Syst. Biol. 56, 564–577.
Thomson, C.M., Herring, P.J., Campbell, A.K., 1995. Coelenterazine distribution and iuciferase characteristics in oceanic decapod crustaceans. Mar. Biol. 124, 197–207.
Toon, A., Finley, M., Staples, J., Crandall, K.A., 2009. Decapod phylogenetics and molecular evolution. In: Martin, J.W., Crandall, K.A., Felder, D.L. (Eds.), Decapod Crustacean Phylogenetics (Crustacean Issues 18). CRC Press, Bocan Raton, FL, pp. 14–28.
Tsang, L.M., Ma, K.Y., Ahyong, S.T., Chan, T.Y., Chu, K.H., 2008. Phylogeny of Decapoda using two nuclear protein-coding genes: origin and evolution of the Reptantia. Mol. Phylogenet. Evol. 48, 359–368.
Vera, J.C., Wheat, C.W., Fescemyer, H.W., Frilander, M.J., Crawford, D.L., Hanski, I., Marden, J.H., 2008. Rapid transcriptome characterization for a nonmodel organism using 454 pyrosequencing. Mol. Ecol. 17, 1636–1647.
Wald, G., 1968. The Molecular Basis of Visual Excitation. Elsevier Publishing Company, Amsterdam, 1972.
Warrant, E.J., Locket, N.A., 2004. Vision in the deep sea. Biol. Rev. 79, 671–712.
Welsh, J.H., Chace, F.A., 1937. Eyes of deep sea crustaceans. Biol. Bull. 72, 57–74.
Whiting, M.F., 2002. Mecoptera is paraphyletic: multiple genes and phylogeny of Mecoptera and Siphonaptera. Zool. Scr. 31, 93–104.
Whiting, M.F., Carpenter, J.C., Wheeler, Q.D., Wheeler, W.C., 1997. The strepsiptera problem: phylogeny of the holometabolous insect orders inferred from 18S and 28S ribosomal DNA sequences and morphology. Syst. Biol. 46, 1–68.
Widder, E.A., 2002. Bioluminescence and the pelagic visual environment. Mar Freshw Behav Phys 35, 1–26.
Widder, E.A., Latz, M.I., Case, J.F., 1983. Marine bioluminescence spectra measured with an optical multichannel detection system. Biol. Bull. 165, 791–810.
Wilson, T., Hastings, J.W., 2013. Bioluminescence: Living Lights, Lights for Living, first ed. President and Fellows of Harvard College, Canada.

Glossary

photophore: a specialized light-emitting organ
opsin: a protein that, when bound to a chromophore, forms a photopigment